

Copyright 2006 Society of Photo-Optical Instrumentation Engineers.

This paper will be published in *Proceedings of SPIE*, Volume 6153, and is made available as an electronic preprint with permission of SPIE. One print or electronic copy may be made for personal use only. Systematic or multiple reproduction, distribution to multiple locations via electronic or other means, duplication of any material in this paper for a fee or for commercial purposes, or modification of the content of the paper are prohibited.

# Two-layer anti-reflection strategies for implant applications

Douglas J. Guerrero<sup>a</sup>, Tamara Smith<sup>a</sup>, Masakazu Kato<sup>b</sup>, Shigeo Kimura<sup>b</sup>, Tomoyuki Enomoto<sup>b</sup>

<sup>a</sup>Brewer Science, Inc., 2401 Brewer Drive, Rolla, MO 65401, USA

<sup>b</sup>Nissan Chemical Industries, Ltd., 635 Sasakura Fuchu-Machi, Toyama-Shi, Toyama, Japan

## ABSTRACT

A two-layer bottom anti-reflective coating (BARC) concept in which a layer that develops slowly is coated on top of a bottom layer that develops more rapidly was demonstrated. Development rate control was achieved by selection of crosslinker amount and BARC curing conditions. A single-layer BARC was compared with the two-layer BARC concept. The single-layer BARC does not clear out of 200-nm deep vias. When the slower developing single-layer BARC was coated on top of the faster developing layer, the vias were cleared. Lithographic evaluation of the two-layer BARC concept shows the same resolution advantages as the single-layer system. Planarization properties of a two-layer BARC system are better than for a single-layer system, when comparing the same total nominal thicknesses.

**Keywords:** BARC, two-layer, wet developable, implant

## 1. INTRODUCTION

Using bottom anti-reflective coatings (BARCs) in implant layers has become more desirable for current technology nodes because tolerances for reflective notching and critical dimension (CD) variations caused by wafer topography are getting smaller. The feasibility of using traditional dry-etch BARCs for implant applications in future technology nodes becomes more challenging because dry-etch BARCs cause more process complexity, more defectivity, and potential substrate damage. A solution to this problem is to eliminate the BARC etch step completely by using a wet-developable BARC. In recent years, wet-developable BARCs have been developed specifically for implant layer applications to replace traditional dry-etch BARC processes.<sup>1-5</sup>

Most wet-developable BARCs utilize a polyamic acid soluble in alkaline media as a polymer binder, thus allowing the BARC to be removed when the resist is developed. These wet-developable BARCs are rendered insoluble in resist solvents because they take advantage of a thermally driven amic acid-to-imide conversion. In some cases, a crosslinker is added to adjust the dissolution rate of the polyamic acid in developer. Although this process works well, it is limited by a thermal bake window and isotropic development behavior. The thermal bake window is defined as the temperature range in which the BARC remains *insoluble* in organic solvents (to avoid intermixing with the resist) but *soluble* in alkaline developer (to allow removal of the BARC). This thermal window is also coupled to the development rate. Development rates decrease as imidization and/or crosslinking reactions take place. Figure 1 illustrates the phenomena.

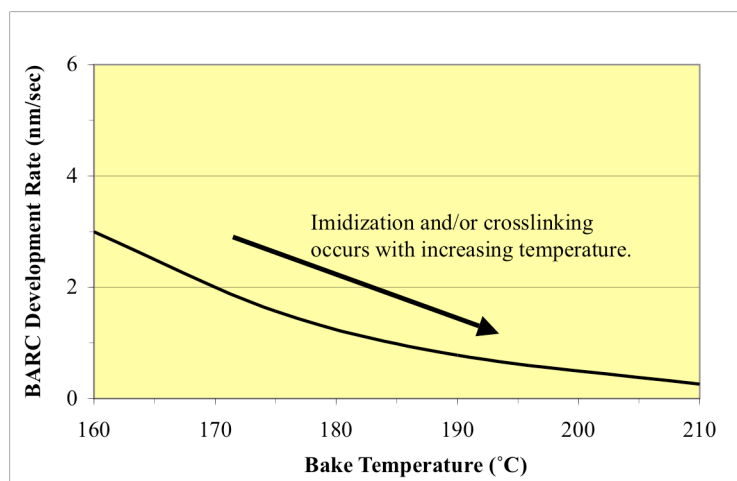


Figure 1. Relationship between BARC development rate and bake temperature.

The combination of thermal control of development rate and isotropic development behavior is problematic because fast development rates at lower temperatures can undercut resist lines, while at high temperatures slow development rates can cause a film to remain after development in between resist lines or in underlying topography. This limitation is further illustrated by using a simple calculation shown in Table I. For the values shown in Table I, we assumed isotropic dissolution behavior, constant development rate from start to finish, and nearly 100% BARC planarization. For example, a BARC having a development rate of 3 nm/sec will require 33.3 seconds to clear a 100-nm-deep via, while the same BARC will require 66.7 seconds to clear a 200-nm via. In a 200-nm or deeper via, this BARC would be expected to leave residue during a standard 60-second development cycle. The areas in gray in Table I show that BARCs with these development rates will require more than 60 seconds to clear topography of various depths.

**Table I.** Calculated development times (in seconds) required to remove BARCs with various development rates from various topography depths.

BARC Dev Rate (nm/sec)	Topography Depth (nm)				
	75	100	150	175	200
1	75.0	100.0	150.0	175.0	200.0
2	37.5	50.0	75.0	87.5	100.0
3	25.0	33.3	50.0	58.3	66.7
4	18.8	25.0	37.5	43.8	50.0
5	15.0	20.0	30.0	35.0	40.0
6	12.5	16.7	25.0	29.2	33.3

Experimentally the above calculations have been demonstrated and are illustrated in Figure 2 below. BARCs with two different development rates were coated on 200-nm vias with features of 150-nm 1:1.5 L/S. After development at various time intervals, the substrates were compared. Figure 2 shows that after developing for 60 seconds, the BARC having a development rate of 1.95 nm/sec did not clear the structures. This BARC required 90 seconds to totally clear the substrate. The second BARC with a development rate of 10 nm/sec totally cleared the substrate in 60 seconds. Our experience has shown that while rates greater than 5 nm/sec are ideal for clearing deep trenches (deeper than 150 nm), such rates are too fast for KrF imaging of features smaller than 0.18 micron.

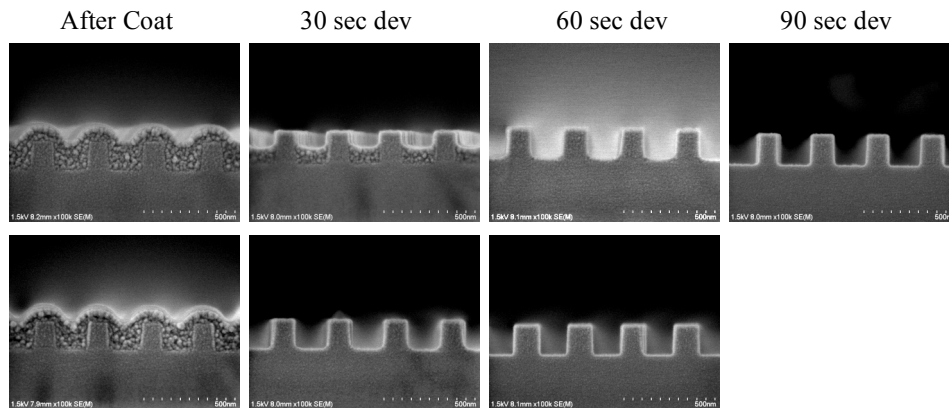


**Figure 2.** SEM cross-section of single-layer BARCs having 1.95 nm/sec (top row) and 10 nm/sec (bottom row) development rates.

Thus it can be said that in an isotropic system, development rate determines the minimum printable CD and time required to remove the BARC from underlying topography. In an ideal case, both goals can be achieved with a single-layer BARC having a given development rate, but in practice, with shrinking CD size and unique topographies, the process becomes more difficult. In this paper we show that by using a two-layer BARC system, which includes a top layer designed with the appropriate development rate for lithography and a second bottom layer for clearing topography, this dilemma can be solved. In addition, planarization advantages can be realized because using two coating layers results in better planarization than using a single coating layer having the same total nominal thickness.

## 2. METHODOLOGY

### 2.0 General

The polymers used in this study were prepared from dianhydrides and diamines condensation reactions using established procedures.<sup>6-8</sup> The polymer solutions were formulated with various amounts of multifunctional epoxide crosslinkers to control dissolution rates. In addition, a DUV dye was added to adjust BARC absorbance. Film thickness on a silicon substrate was measured with a WS-LSE Gaertner ellipsometer. Ethyl lactate was used as a stripper solvent to determine the minimum temperature required for baking the BARC while maintaining solvent resistance after coating and curing. The solvent was allowed to puddle on the film for 20 seconds, and spin dried. The film thickness was compared before and after solvent contact. Most films were sufficiently cured to avoid intermixing at temperatures of 160°C or higher. Optical constants  $n$  and  $k$  were measured at 248 nm using a M2000 Woollam variable-angle spectroscopic ellipsometer.

### 2.1 Development rates

The films were coated and baked on silicon wafers at various temperatures. Development rates were determined using a development rate monitor (DRM) RDA-790 (made by LithoTech) having a bath with PD523AD (0.26N TMAH) developer.

### 2.2 Lithography

The BARC formulations were coated and baked on silicon substrates. The bottom and top layers had thicknesses of 60 and 15 nm, respectively. The two-layer BARC was then coated with TDUR-P338 EM KrF photoresist (post-application bake: 100°C for 90 seconds; post-exposure bake: 110°C for 90 seconds). Exposures were performed with a Nikon S-203B scanner (NA = 0.6,  $\sigma = \frac{1}{2}$  annular) and a binary mask. The wafers were developed using NMD-3 2.38% TMAH at 23°C for 60 seconds and rinsed with water.

### 2.3 BARC removal

The ability of the films to clear out of structures was determined by coating single and two-layer BARCs on vias having depths of 50, 80, 140, and 200 nm. At each given depth, the vias had 1:1 L/S varying from 80–500 nm. The films were coated, baked, and immersed in developer for 60 seconds. Residual film remaining inside vias was measured from SEM micrographs.

### 2.4 Planarization

Planarizing characteristics of single and two-layer BARCs were determined by coating each film on 200-nm deep vias having 160- and 500-nm 1:1 L/S. The single and two-layer BARCs were coated to achieve equivalent total thicknesses. The single-layer BARC was coated and baked at 185°C to give a thickness of 74 nm. The bottom layer of the two-layer BARC system was coated and baked at 185°C to give a thickness of 60 nm. Then the second layer was coated on the bottom layer and baked at 175°C to produce a total film stack of 76 nm. Film planarization from each coating was measured from SEM micrographs.

## 3. DATA AND RESULTS

### 3.1 Development rate control

One of the key parameters affecting the performance of wet-developable polyamic acid-type BARCs is development rate. In order to first determine the desired development rate, a polyamic acid was synthesized and formulated with various amounts of crosslinker. Figure 3 shows the development rate of developable BARCs DB-1 to DB-6 after baking at 175°C. The increasing amounts of crosslinkers are relative to DB-1 such that DB-2 has 10 times the amount of DB-1 and so on. The graph shows that as the crosslinker amount increases, the development rate decreases. For this study, we selected DB-4 as a single-layer BARC, and DB-2 and DB-3 as bottom-layer candidates based on their development rates. The development rates for DB-2, DB-3, and DB-4 were 33, 6.8, and 1.6 nm/sec, respectively.

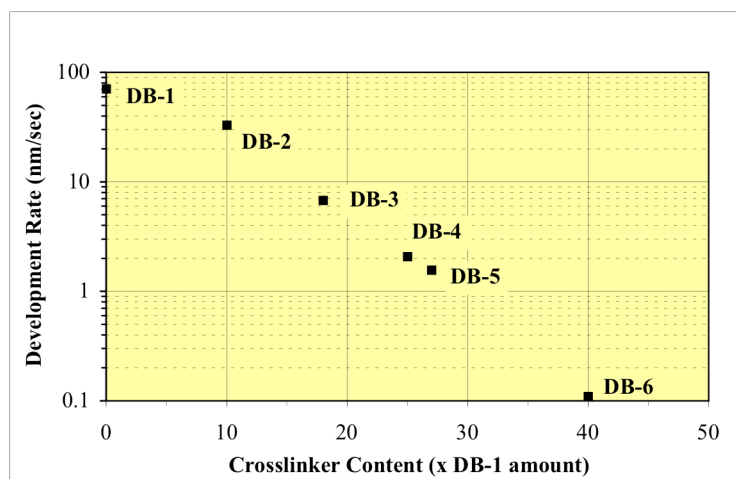


**Figure 3.** Relationship between crosslinker content and development rate after baking films at 175°C.

### 3.2 BARC removal evaluation

Each individual layer selected above was tested for its ability to clear out of vias that were 200 nm deep and 140 nm wide. BARCs DB-2 and DB-3 were coated and baked twice at 165°C and 175°C. The double-bake process was intended to simulate the two bake steps experienced by the bottom layer of the two-layer BARC. DB-4 was baked only once as is normally done for single-layer BARCs. Figure 4 shows the SEM cross-sections of the vias. The SEM micrographs show that single-layer DB-4 BARC is not completely removed from the vias even at the lower bake temperature where a higher development rate is expected. DB-2 was a better candidate for a bottom layer than DB-3 because DB-3 leaves a small amount of residue at 165°C and 175°C. It can be concluded that at each given temperature, the ability of the BARCs to be removed from the vias is related to their corresponding development rates.

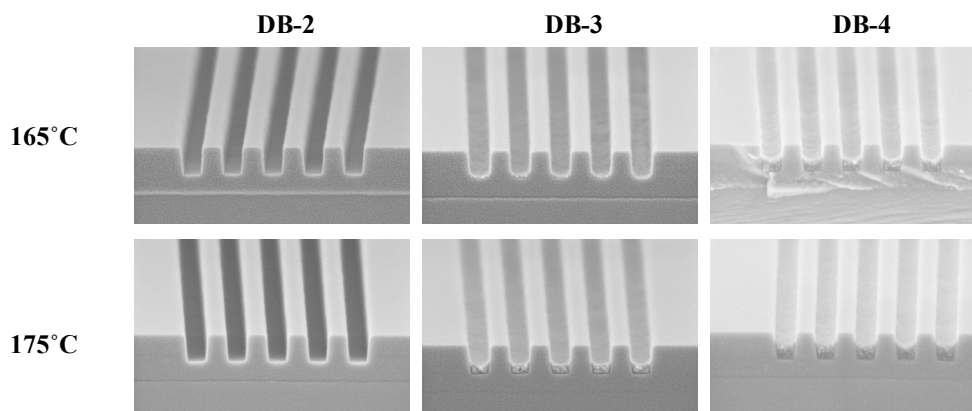


**Figure 4.** Removal evaluation of DB-2, DB-3, and DB-4 BARCs from vias 200 nm deep.

Using the same experimental procedure, the two-layer BARC process was tested by coating DB-4 (slow development rate) on top of each of the two bottom layers (DB-2 and DB-3). The top and bottom layers were baked at 175°C each. Figure 5 shows that after development, the DB-4/DB-2 stack cleared, while the DB-4/DB-3 combination did not. This dramatic result shows that while both layers had similar thicknesses and the same top layer, the ability to clear the vias can be directly attributed to the bottom layer's composition and development rate.

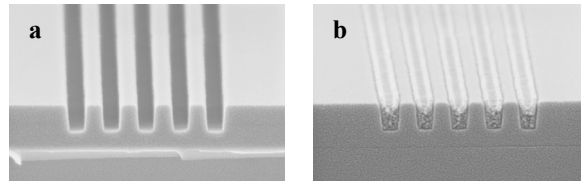


**Figure 5.** Two-layer BARC systems after development: a) DB-4/DB-2 and b) DB-4/DB-3.

### 3.3 Two-layer configuration

We found that crosslinker amounts used to control the BARCs' development rates did not significantly affect the optical properties of the films tested. In the two-layer design, both layers have similar optical properties ( $n$  and  $k$  values), thus, optically they behave as one thick layer of either coating. The question remaining then was which layer should be the thicker layer in a BARC stack having a total thickness of 75-80 nm? Two options were explored: 1) a thin slow-developing layer on top of a thick fast-developing layer, and 2) a thick slow-developing layer on top of a thin fast-developing layer. We coated DB-4 (35 nm)/DB-2 (45 nm) and DB-4 (45 nm)/DB-2 (37 nm) on 200-nm vias and baked each layer at 175°C. Figure 6 below shows the SEM cross-sections of both two-layer systems before and after a 60-second development time. The via cleared in the case where DB-2 filled 47% of the space within the via after coating, while the thinner coating (44% via fill) did not. This observation suggests that the vias must be mostly filled by the faster developing BARC for the dissolution process to be successful within the time limit of the development step.

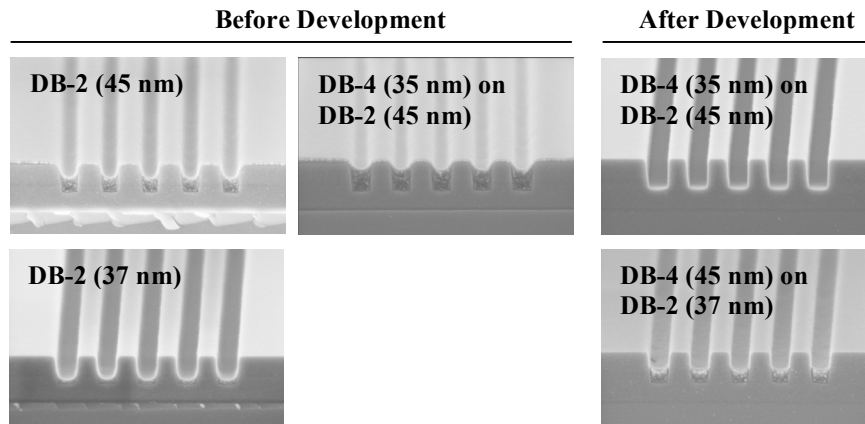


**Figure 6.** Two-layer BARC before and after development of 200-nm vias.

### 3.4 Lithography

The lithographic performance of the two-layer system was evaluated using layers DB-8 on DB-9 under various bake temperature conditions. Film stack DB-8/DB-9 is similar to DB-4/DB-2 except that the former uses a polymer with enhanced edge bead removal solvent compatibility. The BARC bake matrix was necessary to determine the optimum bake conditions for each layer. In the bake temperature matrix, bottom layer DB-9 was cured at 180°C, 185°C and 190°C, and top layer DB-8 at 165°C, 170°C and 175°C. Figure 7 shows the SEM cross-sections of 140-nm L/S (center focus) at these bake conditions.

In the two-layer BARC process, the quality of the printed line is related the amount of crosslinking or “hardness” of each layer. If the surface of the BARC is too “soft,” the resist intermixes with the BARC, which leads to a footing profile. If the surface is too crosslinked, the developer will not remove the BARC, which causes scum. A qualitative degree of crosslinking can be used to describe the lithographic results shown in Figure 7. When the bake temperature of the top layer is at the lowest (165°C), its surface is “soft,” which leads to lines with footing. Undercut is also observed in the large pattern due to the low bake temperature of the DB-9 layer. As the bake temperature of DB-8 is increased, footing and scum disappear, an undercut transition phase occurs at 170°C, and a good profile is obtained at 175°C. When DB-9 bottom layer is processed at 185°C, the same transition is observed. However, good lines are now observed sooner at 170°C top layer bake. The last row in Figure 7 can be explained by the extreme surface hardness differences

that can occur between the BARC layers. When the bottom layer is baked at the highest temperature (190°C) and the top at the lowest (165°C), the mismatch in curing causes stresses and line failure at the BARC layers' interface. The SEM micrograph shows that the bottom BARC layer is still remaining on the substrate, while the two outer lines have collapsed along with the top layer. A compromise to this condition is observed at 170°C/190°C DB-8/DB-9 BARC bake, but when both layers are baked at the highest temperature, the expected scum appears. These results indicate that careful bake temperature optimization between the layers must take place in order to achieve optimum lithography.

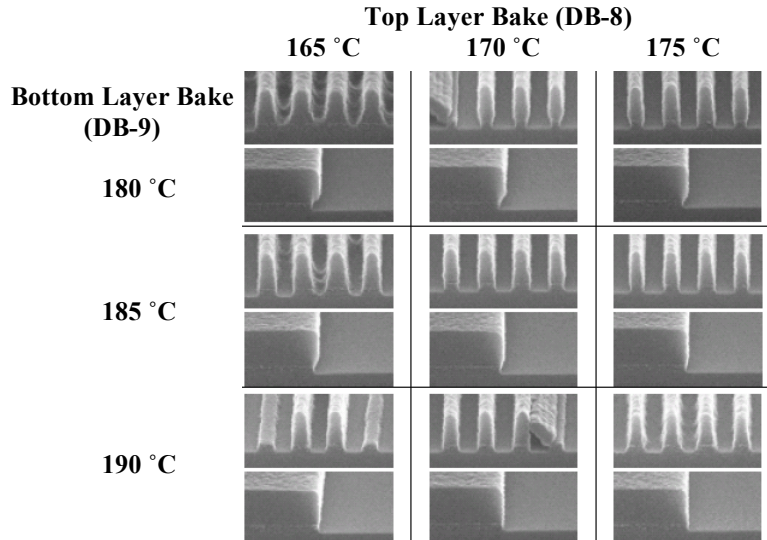
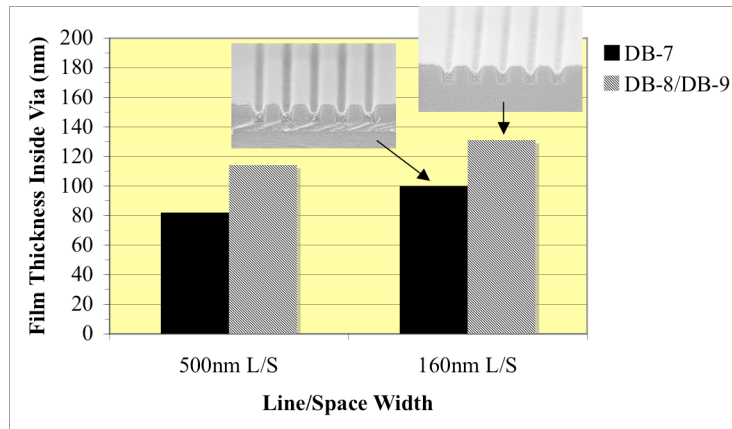


Figure 7. Effect of layer bake conditions on lithographic performance of 140-nm L/S.

### 3.5 Planarization

Substrate planarization provides advantages during the lithography process because it reduces the swing effect due to resist thickness variations.<sup>9</sup> We found that using a two-layer BARC system provides planarization benefits over using a single-layer BARC because a higher degree of planarization can be achieved using the two-layer system, even when applying both types of coatings to produce the same total nominal thickness. The observation can be explained by the filling effect and leveling of topography that takes place when the first of the two layers is applied. We coated and baked the single-layer BARC DB-7 (74 nm) and the two-layer stack made of DB-8 (16 nm)/DB-9 (60 nm) over 200-nm vias. The thickness from the bottom of the substrate to the top of the BARC inside the via was measured using SEM micrographs. The results are shown in Figure 8. The two-layer BARC filled 66% of the vias having 160 nm spaces, while the single-layer BARC filled 50%. The difference was maintained across via pitch. The 500-nm wide vias were filled to 57% with the two-layer BARC system and 41% with the single-layer coating.



**Figure 8.** Via-filling comparison of single-layer and two-layer BARC systems.

#### 4. CONCLUSIONS

A two-layer anti-reflection strategy has been proposed. The two-layer BARC system was compared to a single-layer BARC. The two-layer BARC system allows for better control and tuning of development rates, which in turn controls the ability to be removed from substrate topography after development. Two relative stack thickness configurations were tested. In situations where deep underlying topography is present, the vias or trenches must be mostly filled with the layer that develops faster. Lithographic evaluation shows the ability to print 140 nm L/S and the image quality is correlated to each layer bake condition. Planarization performance of the two-layer BARC system is better than that of the single-layer BARC.

#### ACKNOWLEDGMENTS

The authors would like to thank John Thompson and Denise Howard for SEM analysis. Tokyo Ohka Kogyo, Co. is gratefully acknowledged for the lithography evaluation of the two-layer BARCs.

#### REFERENCES

1. Y.H. Lim, Y.K. Kim, J.S. Choi, and J.G. Lee, "Process optimization of developer soluble organic BARC and its characteristics in CMOS devices," *Proceedings of SPIE*, vol. 5753, 2005, pp. 690-698.
2. I. Guilmeau, A. Guerrero, V. Blain, S. Kremer, V. Vachellerie, D. Lenoble, P. Nogueira, S. Mougél, and J.-D. Chapon, "Evaluation of wet-developable KrF organic BARC to improve CD uniformity for implant application," *Proceedings of SPIE*, vol. 5376, 2004, pp. 461-470.
3. X. Shao, A. Guerrero, and Y. Gu, "Taking the wet-developable route to applying BARC in implant layers," *Solid State Technology*, vol. 47, no. 6, 2004, pp. 61-64.
4. C. Cox, D. Dippel, C. Ghelli, P. Valerio, B. Simmons, and A. Guerrero, "Developer Soluble Organic BARCs for KrF Lithography," *Proceedings of SPIE*, vol. 5039, 2003, pp. 878-882.
5. D.J. Guerrero and T. Trudgeon, "A New Generation of Bottom Anti-Reflective Coatings (BARCs): Photodefinable BARCs," *Proceedings of SPIE*, vol. 5039, 2003, pp. 129-135.

6. J. Kruse, J. Kanzow, K. Ralitzke, F. Faupel, M. Heuchel, J. Frahn, and D. Hofmann, "Free Volume in Polyimides: Positron Annihilation Experiments and Molecular Modeling," *Macromolecules*, vol. 38, 2005, pp. 9638-9643.
7. R. C. Cox and C. J. Neef, "Spin bowl compatible polyamic acids/imides as wet developable polymer binders for anti-reflective coatings," U.S. Pat. Appl. Publ. 20040210034 A1, 2004.
8. S.L.-C. Hsu, P.-I. Lee, J.-S. King, and J.-S. Jeng, "Synthesis and Characterization of a Positive-Working, Aqueous-Base-Developable Photosensitive Polyimide Precursor," *Journal of Applied Polymer Science*, vol. 86, 2002, pp. 352-358.
9. A.H. Gabor, S.D. Halle, and C. Kallingal, "Topography Impacts on Line-width Control for Gate Level Lithography," *Proceedings of SPIE*, vol. 5753, 2005, pp. 699-707.